Supplementary Information

3D PRINTED MULTIMATERIAL MICROFLUIDIC TRANSISTORS

Alireza Ahmadianyazdi[¥,1], Wei Huang[¥,1,2], Kaustav A. Gopinathan[¥,3], Ivan Stepanov[*,1,4], Ting-Yuan Tu[2], Mehmet Toner[3,5], and Albert Folch[1]

[1]Department of Bioengineering, University of Washington, Seattle, WA, 98195

[2] Department of Biomedical Engineering, College of Engineering, National Cheng Kung University, Tainan 70101, Taiwan (R.O.C)

[3]Center for Engineering in Medicine & Surgery, and Department of Surgery Massachusetts General Hospital, Boston, MA 02114

[4]Department of Mechanical Engineering, University of Washington, Seattle, WA, 98195

[5]Shriners Children's, Boston, MA 02114

[*]Corresponding author, e-mail address: steiva@uw.edu

[¥]These three authors contributed equally to this work

S1. First-order mechanistic model of flow limitation in a microfluidic valve

In our transistors, the fluid height at the valve is variable and has a maximum value $H = 80$ μm, and its width $\omega = 800$ μm is constant. In the elastic regime, the membrane deflection at the center of the membrane d is proportional to the transmembrane pressure $P_{GM} \equiv P_G - P_M$:

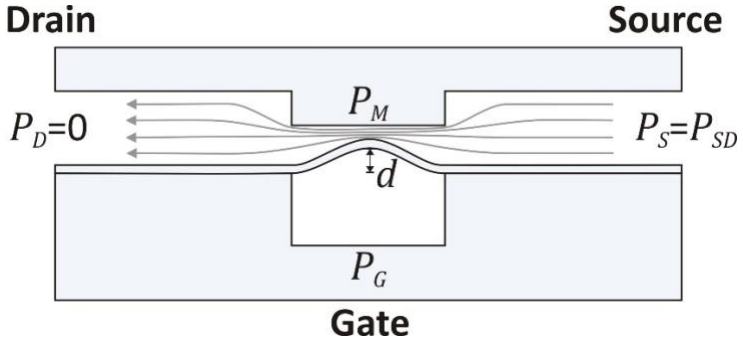

$$d = kP_{GM} \ , \ k > 0 \ \text{(elastic regime)}$$

where k is a function that embodies the membrane's materials and dimensions. For most materials, k is a function of P_{GM} (tends to decrease for larger deflections) that is difficult to express analytically for large pressure values, but it is *measurable* (by measuring d), so for now we write $k = k(P_{GM})$.

Here we assume that the pressure at the drain P_D is 0, that the valve length L is small compared to the distance between source and drain, and that the device is symmetrical (so the valve is in

the middle of the transistor). Therefore, the pressure at the valve seat P_M is approximately $P_S/2$, where P_S is the pressure applied at the source. Thus,

$$d = k(P_G - P_S/2)$$

Since $P_{GS} = P_G - P_S$ = ct. (operating condition of the transistor), we can also write $k = k(P_{SD})$. In addition, because $P_D = 0$, we can use $P_S = P_{SD}$ and obtain:

$$d = k(P_G - P_S + P_S/2) = k(P_{GS} + P_S/2) = k(P_{GS} + P_{SD}/2)$$

The bending membrane forms a domed constriction in the valve seat whose exact hydraulic resistance is difficult (if not impossible) to calculate analytically. Since our goal is to obtain a first-order mechanistic understanding of *why* flow limitation arises, and the transistor's behavior is only dictated by the hydraulic resistance, we approximate our gate by an imaginary "smart spigot" whose fluid path for any given applied P_G has the same hydraulic resistance as the real membrane at that P_G:

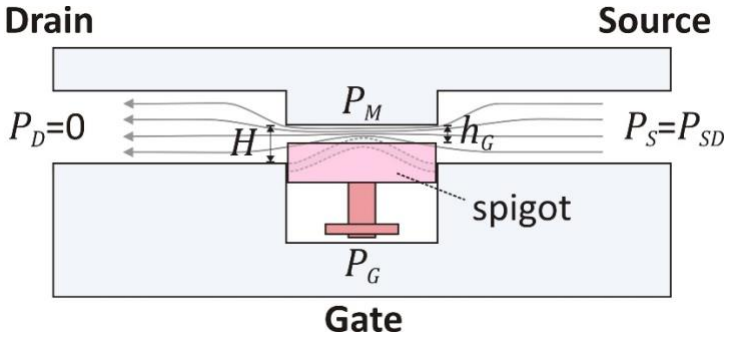

In our spigot, the fluidic path of the gate has a rectangular shape of height h_G that can be approximated as:

$$h_G \approx H - d = H - k(P_{GS} + P_{SD}/2)$$

where $k = k(P_{SD}, P_{GS})$ "encodes" the membrane's physical characteristics (including thickness and Young's modulus) and elastic behavior (including non-linear dependences with P_{SD} and P_{GS}) so as to produce the average hydraulic resistance of the original gate at this P_{SD}. We expect that, as P_{SD} increases, the material will become stiffer so *k* will decrease.

Conveniently, the gate's resistance in our spigot model can be approximated using the Navier-Stokes solution for viscous flow in a rectangular channel:

$$R_G \approx \frac{12\eta L}{\omega h_G^3 (1 - 0.63\, h_G/\omega)} \quad \text{(Eqn. 1)}$$

Where η is the fluid's viscosity and L and ω are the valve length and width, respectively. Note that $0 < h_G < H$ and that, in our transistors, $H \approx \omega/10$, therefore:

$$R_G \approx \frac{12\eta L}{\omega h_G^3}$$

To evaluate the term h_G^3 , we substitute:

$$h_G^3 = (H - k(P_{GS} + P_{SD}/2))^3 = H^3\left(1 - \frac{k}{H}\left[P_{GS} + \frac{P_{SD}}{2}\right]\right)^3$$

where the term $(1 - k/H\,(P_{GS} + P_{SD}/2))$ is always positive because $0 < h_G < H$. In other words, the function $k = k(P_{SD}, P_{GS})$ can never exceed the value $H/(P_{GS} + P_{SD}/2)$ for all pressure values.

Note that the term $12\eta L/\omega H^3$ is the value of R_G for P_{SD} = 0, so we denote it with $R_G(0)$ for simplicity. In general, the (passive) fluidic resistance of the channel R_{ch} differs from $R_G(0)$ by a constant C that is always known, *i.e.*, $R_{ch} = R_G(0)/C$. For our geometries, C = 1.35 = 1/0.743 (see main text).

We are interested in evaluating $Q_D = P_{SD}/(R_{Ch}+R_G)$, where $R_G = f(P_{SD})$. Thus,

$$Q_D(P_{SD}) = \frac{P_{SD}}{R_{Ch} + R_G} = \frac{P_{SD}}{\frac{R_G(0)}{C} + \frac{12\eta L}{\omega H^3\left(1 - \frac{k}{H}\left[P_{GS} + \frac{P_{SD}}{2}\right]\right)^3}}$$

Simplifying,

$$Q_D(P_{SD}) = \frac{1}{R_G(0)}\frac{P_{SD}}{\frac{1}{C} + \frac{1}{\left(1 - \frac{k}{H}\left[P_{GS} + \frac{P_{SD}}{2}\right]\right)^3}}$$

Substituting the values of $R_G(0)$ and C, we obtain for our transistor:

$$Q_D(P_{SD}) = \frac{\omega H^3}{12\eta L}\frac{P_{SD}}{0.743 + \frac{1}{\left(1 - \frac{k}{H}\left[P_{GS} + \frac{P_{SD}}{2}\right]\right)^3}} \quad \text{(Eqn. 2)}$$

Redefining $x \equiv P_{SD}$, $f(x) \equiv R_G(0)Q_D(P_{SD})$, and $a(x) \equiv k(P_{SD})/2H$, we obtain for the case $P_{GS} = 0$:

$$f(x) = \frac{x}{0.743 + \frac{1}{(1 - a(x)x)^3}}$$

Note that the spigot model (Eqn. 1) is both an approximation and a subterfuge that allows us to "encode" the membrane characteristics (i.e. thickness and Young's modulus) and behavior into the $k(P_{SD})$ function (or, equivalently, the *a(x)* function), which is valid for all P_{SD} values and ultimately is only a function of P_{SD}. We can use graphing software to simulate the function $Q_D(P_{SD})$ for various $k(P_{SD}, P_{GS})$ functions. In the (unrealistic) elastic case, $k(P_{SD}, P_{GS})$ = ct., the function $Q_D(P_{SD})$ has a shape that is clearly linear for small P_{SD} but does not reproduce the flow limitation behavior for large P_{SD} (see **Fig. 1**E for $a(x) = 0.05$ [in psi^{-1} if P_{SD} is in psi]).

On the other hand, for a $k(P_{SD}, P_{GS} = ct.)$ function that decreases linearly by about 40% of its initial (elastic-case) value as P_{SD} increases in the range of pressures considered (a more realistic assumption, as the stiffness of most elastic materials increases with deformation), we obtain a more experimentally-realistic "flattening shape" at large P_{SD} while maintaining the same linear slope at small P_{SD} (see **Fig. 1**F for $a(x) = 0.05 - 0.00125x$, which decreases from $a(0) = 0.05$ to

$a(15)$ = 0.03125, a 62.5% of its initial value). For the case $k(P_{SD})$ = 0 (a rigid membrane), Eqn. 1 correctly simplifies to $Q_D = P_{SD}/(R_{Ch}+R_G(0))$, which is the classical form of flow rate-pressure relation in a microchannel with rigid walls. We stress that our first-order formula fails to predict flow limitation ($Q_D(P_{SD}) \sim ct.$) for extremely large P_{SD}, or $x \rightarrow \infty$, and instead it yields $Q_D(P_{SD}) \rightarrow \infty$ unrealistically (a failure that is not uncommon in first-order analyses). Importantly, the shape of this curve is very sensitive to H (the vertical dimension of the valve) and to the initial value and slope of $k(P_{SD}, P_{GS})$ (*i.e.*, to the stretchability of the membrane), which explains why a high-resolution manufacturing technique is required for these devices.

Recall that Eqn. 2 was derived assuming

$$d = kP_{GM} \ , \ k > 0$$

but making no assumptions on the functional dependence $d(x,y)$ across the membrane. It is interesting, as shown below, that Eqn. 2 can be derived by approximating the membrane height $d(x,y) \sim d(x)$ by the analysis of beam deflections under a uniform pressure distribution with fixed constraints on both sides:

$$d(x) \approx \frac{P_{GM}}{2Et^3}x^2(L-x)^2$$

where E, t and L are the elastic modulus, the thickness, and the length of the membrane, respectively. Note that $d(x)$=0 both for x=0 and x=L.

The average of $d(x)$ over the whole length of the valve is:

$$\bar{d} = \frac{1}{L}\int_0^L d(x)dx = \frac{P_{GM}}{2LEt^3}\int_0^L x^2(L-x)^2dx = \frac{P_{GM}}{2LEt^3}\frac{L^5}{30} = \frac{P_{GM}L^4}{60Et^3}$$

where we can substitute

$$P_{GM} = P_{GS} + P_{SD}/2$$

We are interested, as before, in evaluating $Q_D = P_{SD}/(R_{Ch}+R_G)$, where

$$R_{ch} = 0.734\, R_G(0) \qquad ; \qquad R_G \approx \frac{12\eta L}{\omega h_G^3}$$

and

$$h_G \approx H - \bar{d} = H - \frac{L^4}{60Et^3}(P_{GS} + P_{SD}/2) = H\left(1 - \frac{K}{H}(P_{GS} + P_{SD}/2)\right)$$

where

$$K \equiv \frac{L^4}{60Et^3}$$

Thus,

$$Q_D(P_{SD}) = \frac{P_{SD}}{R_{Ch} + R_G} = \frac{P_{SD}}{0.734\ R_G(0) + \dfrac{12\eta L}{\omega H^3 \left(1 - \dfrac{K}{H}\left[P_{GS} + \dfrac{P_{SD}}{2}\right]\right)^3}} \quad \text{(Eqn. 3)}$$

Since, again, the term $12\eta L/\omega H^3$ is the value of R_G for P_{SD} = 0, the above equation is equivalent to Eqn. 2, which leads to flow limitation. In other words, the "spigot model" assumption is equivalent to averaging the fluid flow over the gate in the case of a membrane approximated as a beam deflecting under a uniform pressure with fixed constraints. Eqn. 3 helps explain (through the expression of K) why experimentally flow limitation is found to be so sensitive to variations in L and t, requiring in the future high-precision manufacturing techniques.

Our model can be characterized as a particular derivation for rectangular channels of the more general "tube law" for deformable cylindrical tubes by Wilson et al.[1] and others.[2–5] Studying the fluid mechanics of the lung, Wilson et al. extended the work of Shapiro[6] and showed that flow limitation in a deformable tube occurs when the tube deforms sufficiently enough so that the local velocity of the fluid at the pinch point exceeds the "critical wave speed" for the system, demonstrating the existance of a viscous limit even in the case of air. The ratio of those two velocities is sometimes termed the Shapiro number.[7] In rigid tubes, it is well-known that greater pressure heads across the tube produce higher flow rates (according to the Poiseuille equation). However, in deformable tubes, Wilson et al. identified two distinct phenomena that counter balance this positive relationship between pressure and flow, and produce the non-linear phenomenon of flow-limitation. Firstly, any small initial deflection in the tube leads to a higher fluid velocity at that constriction, which reduces the static pressure via the Bernoulli principle and acts to constrict the tube further, thereby choking flow. This phenomenon is analyzed by Shapiro in his seminal paper and applies to inviscid flows.

Wilson et al. also identified a second phenomenon, where a small initial constriction in a tube produces viscous losses in the fluid, which reduces the downstream pressure and acts to constrict the tube further, again choking flow. While this phenomenon was not directly studied by Shapiro, Wilson et al. showed that depending on the geometry and flow conditions, deformable tubes can experience one or both of these phenomena, either of which leads to pinching and therefore flow-limiting behavior, even as P_{SD} tends to infinity.[1] Gopinathan et al. demonstrated that flow limitation in their PDMS microfluidic transistors were accurately predicted with a simple model of the first phenomenon in flat channels rather than tubes. Here, we consider the viscous effects of the second phenomenon as well and extend the mathematical model of flow limitation in microfluidic transistors to account for viscous effects in rectangular channels. The "water spigot" analogy (on which our linear approximation is based) commonly used for describing electronic p-JFETs is very useful for explaining the saturation behavior because it is immediately extrapolatable to microfluidic transistors. Electronically, the saturation in I_D as V_{SD} increases is caused by the narrowing of the electronic path due to the creation of the depletion regions within the channel of the p-JFET. In the microfluidic transistor, the saturation in Q_D as the flow-driving P_{SD} increases (known as "flow limitation") is caused by the narrowing of the fluidic path due to the bending of the elastomeric membrane (by P_G = P_{SD}/2) in the valve region of the microfluidic transistor.

S2. Alternative expression for the Shapiro number *S*

Gopinathan et al.[8] derived S for their PDMS microfluidic transistors as:

$$S = Q\left(\frac{A^3\pi^4 t^3}{6\rho W^5}\frac{E}{1-v^2}\right)^{-\frac{1}{2}}$$

Where Q is the flow rate, A is the cross-sectional area, t is the membrane thickness, W is the width of the microchannel, ρ is the liquid density, E denotes elastic modulus, and v represents Poisson's ratio. By approximating $A \approx W \times H$ and $Q \approx U \times W \times H$ (where U is the average flow velocity), and replacing them in the above equation, an alternative expression for S can be found:

$$S \approx U\left(\frac{\pi^4 H t^3}{6\rho W^4}\frac{E}{1-v^2}\right)^{-\frac{1}{2}}$$

For a given microchannel geometry, $S \approx U/\sqrt{E}$, so highly elastic materials (*i.e.*, very small E) must be used to achieve flow limitation ($S > 1$) with the low flow velocities that are typical of microfluidics.

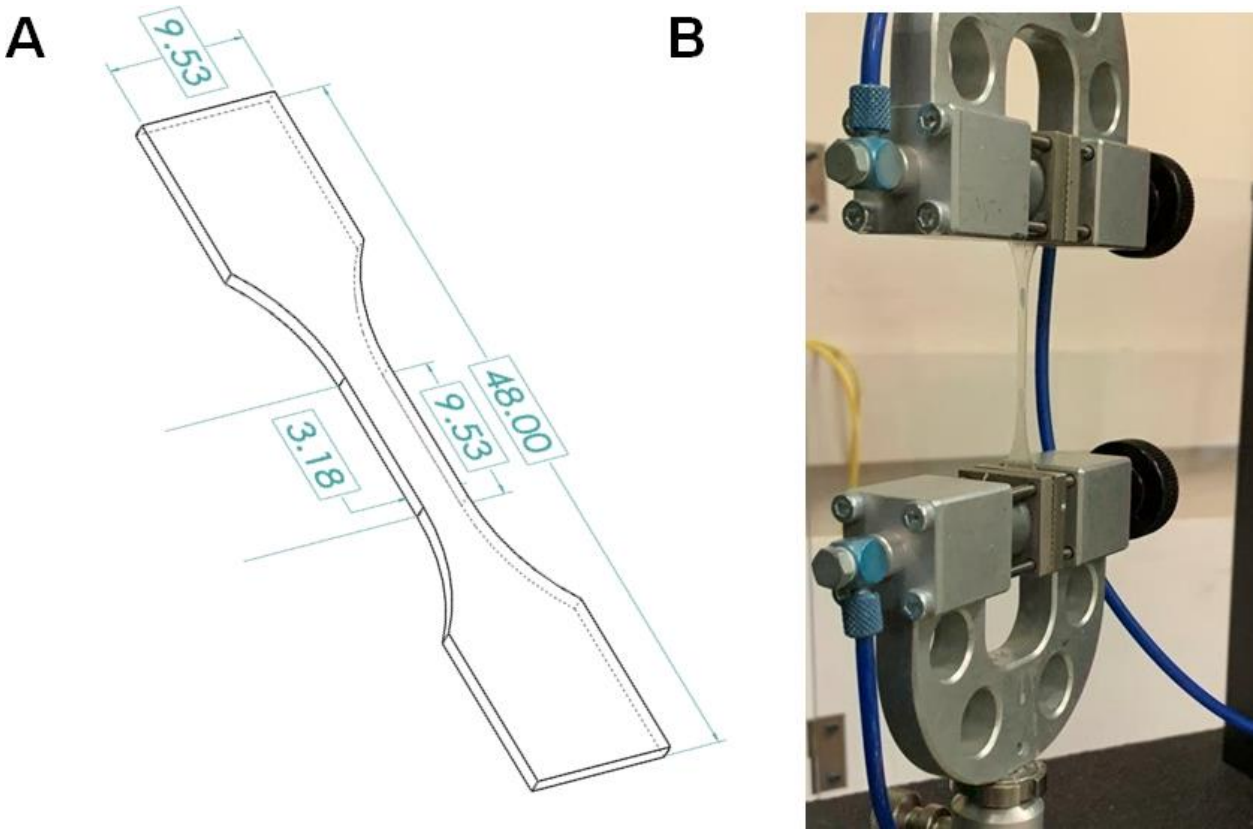

Fig. S1. A. Schematic of the dog-bone specimen for measurement of mechanical properties of HEA-*co*-PPGDA and PDMS. The dimensions are in millimeters. **B.** Stretchability of 85% HEA in Instron load frame.

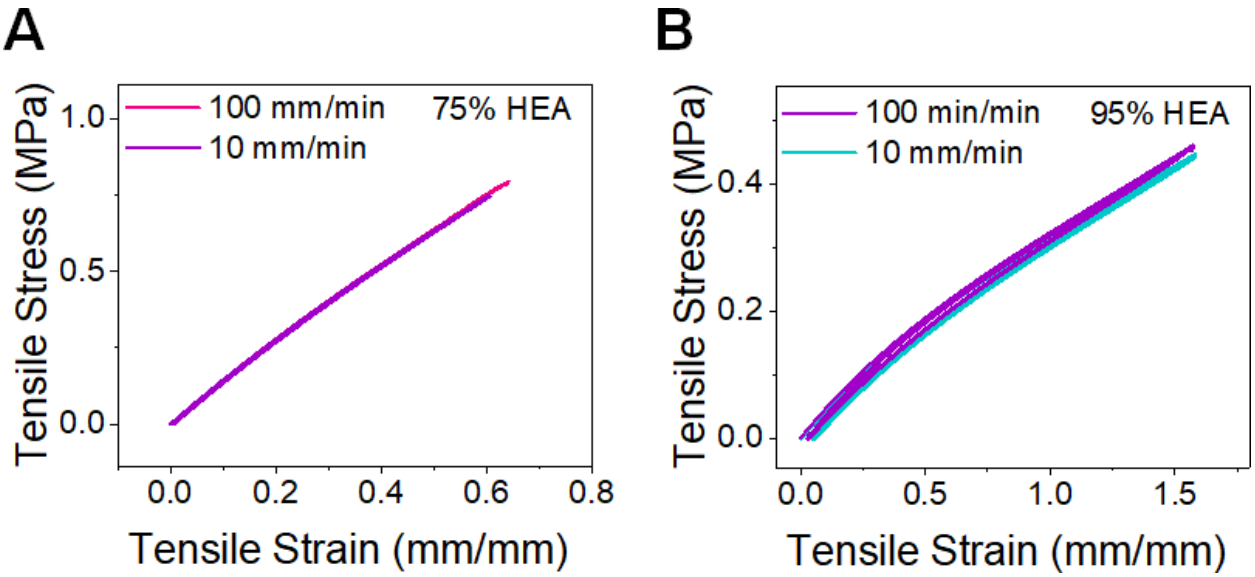

Fig. S2. Dynamic mechanical response of 75% (**A**) and 95% (**B**) HEA dog-bone specimen.

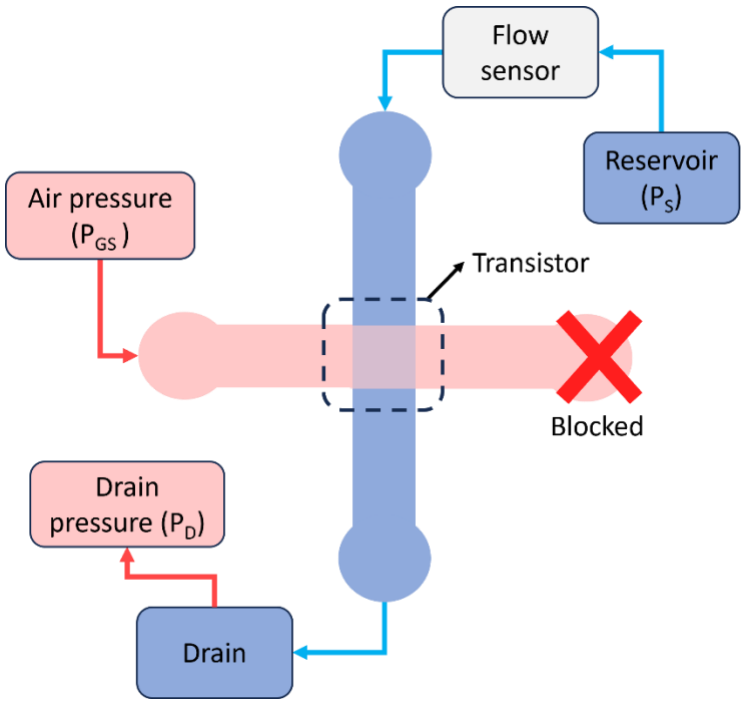

Fig. S3. Schematic of the experimental setup to test the SLA-printed microfluidic transistor.

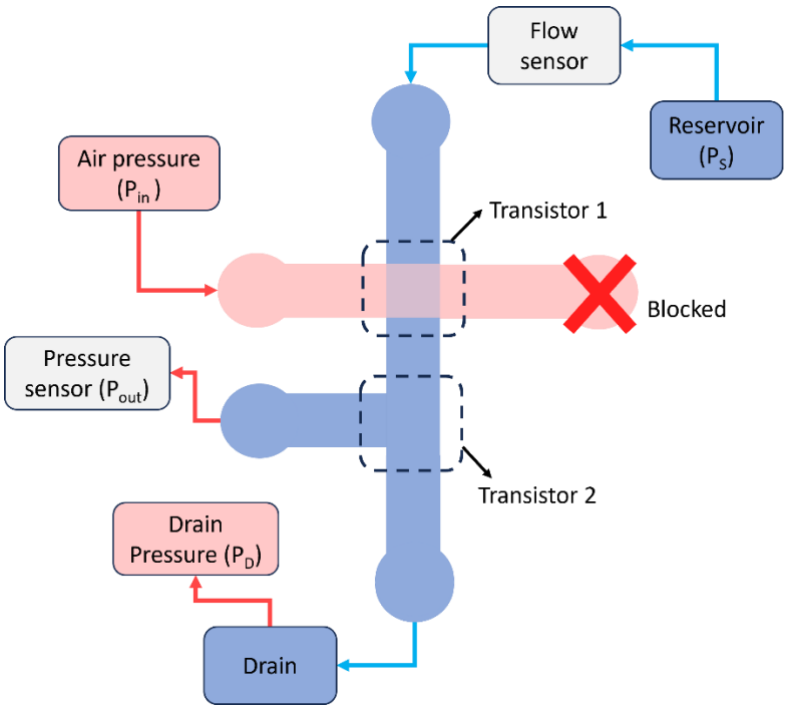

Fig. S4. Schematic of the experimental setup to test the SLA-printed microfluidic analog pressure amplifier.

REFERENCES

1. Wilson, T. A., Rodarte, J. A. & Butler, J. P. Wave-speed and viscous flow limitation. in *Handobook of Physiology: The Respiratory System. Vol. 3* (eds. Macklem, P. & Mead, J.) 55–61 (American Physiological Society, Baltimore, MD, USA, 1986).
2. Kamm, R. D. & Pedley, T. J. Flow in collapsible tubes: a brief review. *J. Biomech. Eng.* **111**, 177–179 (1989).
3. Matsuzaki, Y., Ikeda, T., Kitagawa, T. & Sakata, S. Analysis of Flow in a Two-Dimensional Collapsible Channel Using Universal “Tube” Law. *J. Biomech. Eng.* **116**, 469–476 (1994).
4. Whittaker, R. J., Heil, M., Jensen, O. E. & Waters, S. L. A rational derivation of a tube law from shell theory. *Quarterly journal of mechanics and applied mathematics* **63**, 465–496 (2010).
5. Anand, V. & Christov, I. C. Revisiting steady viscous flow of a generalized Newtonian fluid through a slender elastic tube using shell theory. *ZAMM Zeitschrift fur Angewandte Mathematik und Mechanik* **101**, e201900309 (2021).
6. Shapiro, A. H. Steady Flow in Collapsible Tubes. *Journal of Biomechanical Engineering* **99**, 126–147 (1977).
7. Païdoussis, M. P. Wave propagation in physiological collapsible tubes and a proposal for a Shapiro number. *Journal of Fluids and Structures* **22**, 721–725 (2006).
8. Gopinathan, K. A., Mishra, A., Mutlu, B. R., Edd, J. F. & Toner, M. A microfluidic transistor for automatic control of liquids. *Nature* **622**, 735–741 (2023).